1961

Isolation and investigation of a lime - montmorillonite reaction product

George Harrison Hilt
Iowa State University

ISOLATION AND INVESTIGATION OF A LIME - MONTMORILLONITE REACTION PRODUCT

by

George Harrison Hilt

A Dissertation Submitted to the
Graduate Faculty in Partial Fulfillment of
The Requirements for the Degree of
DOCTOR OF PHILOSOPHY

Major Subject: Civil Engineering

Approved:

Signature was redacted for privacy.

In Charge of Major Work

Signature was redacted for privacy.

Head of Major Department

Signature was redacted for privacy.

Dean of Graduate College

Iowa State University
Of Science and Technology
Ames, Iowa

1961

TABLE OF CONTENTS

INTRODUCTION

Background

During the past decade the supply of natural gravels and rock suitable for crushing has dwindled considerably in many sections of the country. Thus, substitutes for these natural materials have been sought after and used in road base construction. Two additives that have been used extensively because of their effectiveness and cheapness are portland cement and lime.

Both of these materials have been tested extensively in a practical manner to determine their efficiency in the stabilization of various soils. Portland cement has also been thoroughly and repeatedly investigated to determine the mechanisms by which cementation occurs.

However, little has been done to determine the basic mechanisms by which lime stabilizes a soil. Rather, research has, for the most part, been primarily concerned only with the physical effects produced by these mechanisms.

Objective

The objective of this paper is, then, to investigate one phase of the mechanisms producing cementation by attempting to isolate and determine the properties of a crystalline reaction product associated with the action of lime with clay.

From the results obtained in this research, other research has developed in exploring additional crystalline products and is now being

pursued at the Iowa Engineering Experiment Station Soil Research Laboratory. When this research is completed and the information is evaluated it is expected that the relationships involved in the formation of new products and the breakdown of the original clay lattice can be determined.

Procedures

During previous research by this writer it was noted that mixes of lime and a soil rich in montmorillonitic clay mixed with water above the liquid limit would within a couple of days apparently be dried below the liquid limit with no loss in weight. In order to determine what was occurring, a portion of this sample was subjected to x-ray diffractometer analysis. Strong indications of a new reaction product were observed but the product could not be found under the microscope.

The research to be undertaken was then (1) to investigate various lime-soil-water systems varying each of the three parameters one at a time to determine the best phase relationships for growing euhedral crystals of large enough size to be observed under the microscope, (2) to isolate these crystals, and (3) to determine their physical and chemical properties.

The first of these was accomplished by preparing a large number of mixtures and allowing them to cure for periods from two days to eight months before examination. Isolating the crystals was done under the microscope and the determination of their properties was undertaken primarily by microscopic and x-ray methods.

REVIEW OF LITERATURE

Effects of Lime on Clay

Much has been published on the desirable effects of adding lime to a soil rich in clay. The National Lime Association (21) reports that the addition of lime to over-wet clayey soils appears to dry them and materially improve their workability. Publications (17) of the Iowa State University Engineering Experiment Station Soil Research Laboratory show favorable results of increasing strength of soils with the addition of lime and lime-fly ash.

The basic mechanisms have been explained by Davidson and Handy (8). First, calcium ions cause a reduction in plasticity of cohesive soils so they become more friable and more easily worked. The mechanism is either a cation exchange or a crowding of additional cations onto the clay, both processes acting to change the electrical charge density around the clay particles. Clay particles then become electrically attracted to one another, causing flocculation or aggregation. The clay, now occurring as aggregates, behaves like a silt, which has a low plasticity or cohesion. A second chemical action which occurs is a carbonation of lime by carbon dioxide of the air producing calcium carbonate, a weak cement and deleterious to overall strength gains. A third class of reactions, termed pozzolanic reactions, results in a slower, long term cementation of compacted mixtures of lime and soil. Pozzolanic reactions apparently involve interactions between hydrated lime and siliceous and aluminous minerals in the soil. It is this latter class of reactions with which

the research to be described in succeeding portions of this paper is concerned.

Clare and Cruchley (6) found that in a clayey soil, lime contents of 1% and less produce a metastable state, but when lime contents greater than that are used, the flocculation of the clay particles is of a more permanent and progressive nature. Calcium silicate and aluminate formed by chemical breakdown of the clay lattice material contribute to flocculation by bonding adjacent soil particles. Ionic flocculation and silicate bonding commence at the same time, the former being an immediate effect while the latter takes a considerable time to complete.

Crosby (7), as a result of laboratory tests on two soils of high clay content, concluded that no appreciable pozzolanic reactions can take place between lime and fly-ash until lime is present in excess of the cationic requirements of the soil. Hilt and Davidson (11) determined what these requirements (termed lime fixation capacity) were for various soils and concluded that for montmorillonitic and kaolinitic soils the fixation capacity occurred at the lime content at which the plastic limit reached a maximum; they found that up to this capacity no increases in strength occurred but that after fixation was complete, pozzolanic reactions occurring with further additions of lime caused significant increases in strength.

Calcium Aluminates and Silicates

Wells, Clarke, and McMurdie (25) have done a great deal of research on the calcium aluminate hydrates. They found that the hexagonal di- and

tetracalcium aluminate hydrates exist only as metastable phases in the system $CaO-Al_2O_3-H_2O$ between 21° and 90°C. The stable phases in this system are gibbsite ($Al_2O_3:3H_2O$), the isometric tricalcium aluminate hexahydrate, and calcium hydroxide. However, the conversion from the metastable to the stable states is a very slow process at the lower temperature but increases in rapidity as the temperature increases. They further showed that no hexagonal tricalcium aluminate existed as such, but rather that crystals approaching this composition or any other between the di- and tetracalcium aluminates were, in fact, intercrystallization between these two phases which can occur because of the similar structure parallel to the a axis. Wells also gives x-ray, optical, and physical properties of these aluminates.

Bessey (2) prepared a tetracalcium aluminate containing about 1.8 percent of carbon dioxide in solid solution which may influence the structure of the compound somewhat and alter its properties accordingly. Roberts agrees that the x-ray patterns with a longest basal spacing of 7.6 Å previously believed to be forms of the di- tri- or tetracalcium aluminate hydrates, really result from the compound $3CaO \cdot Al_2O_3 \cdot CaCO_3 \cdot 12H_2O$ which is readily formed when the tetra- and di-calcium aluminate hydrates are exposed to atmospheric carbon dioxide. He further found that the two forms of the 13 H_2O hydrate of tetracalcium aluminate characterized by longest x-ray basal spacings of 8.2 Å and 7.9 Å, are polymorphs which occur because of slight differences in packing in the crystal lattice.

Michel and Buser (19) theorize that the calcium aluminate hydrates are composed of alternate layers of calcium hydroxide and aluminum hydroxide.

Other complex anions may occur in the alumina layer which changes the basal spacing depending on the nature of the anion.

Heller and Taylor (10) compiled much of the available information on the calcium silicates listing many of their chemical, physical, and x-ray properties. Most of these are of orthorhombic or lower symmetry.

MATERIALS

Soils

Five soils were used in this investigation. The choice of these soils was based on the type, purity and amount of the principal clay mineral present, and on the availability of the soil. Each of these soils is identified by a letter designating the principal clay mineral and a number indicating the percentage content of the soil less than two microns in diameter. For example, the designation, M-75, indicates a soil containing montmorillonite as the principle clay mineral with 75% of this soil less than 2 microns in effective diameter.

The locations from which these soil samples were taken and other pertinent information appear in Table 1. Table 2 gives the physical and chemical properties of these soils.

Clays

Two different clays were used, one a bentonite and the other a kaolinite. These particular clays were selected because they contained only small amounts of impurities. Information concerning them are contained in Tables 1 and 2.

Table 1. Soil site characteristics

Sample	Location	Classification	Soil series and horizon	Sampling depth, in.
M-67	Keokuk County, Iowa	Post Kansan paleosol ferreto	Mahaska, fossil B horizon	91-101
M-51	Harris County, Texas	Coastal plain deposit, largely deltaic	Lake Charles, probably B horizon	39-144
I-44	Monroe County, Michigan	Probably Wisconsin-age glacial till	Unknown series, probably C horizon	Unknown
I-41	Livingston County, Illinois	Wisconsin-age glacial till	Clarence, C horizon	46-56
K-30	Durham County, North Carolina	Residual soil over medium grained biotite granite	Durham, B horizon	24" below bottom of A horizon
Bentonite	Otay, California	Pliocene age, transported altered ash	San Diego formation	120-216
Kaolinite	Bath, South Carolina	Cretaceous age	Upper Hamburg formation	40-100 ft.

Lime

Reagent grade calcitic hydrated lime, $Ca(OH)_2$, was used to minimize compositional variables. Individual one pound bottles of lime were kept sealed until immediately before use to prevent carbonation of the lime by carbon dioxide in the air. An analysis of the lime is in Table 3.

Table 2. Properties of soils and clay

Sample	M-67	M-51	IC-44	IC-41	K-30	Bentonite
I.E.E.S. designation	528-8	AR-3	AR-4	AR-8	AR-6	---
Textural composition[a], %						
Gravel (> 2mm)	0.0	0.0	0.0	0.0	0.0	
Sand (2-0.074mm)	16.6	3.0	7.0	10.0	45.2	
Silt (74-5μ)	15.5	36.0	36.0	38.0	18.3	
Clay (< 5μ)	70.5	61.0	57.0	52.0	36.5	
Clay (< 2μ)	67.0	51.0	44.0	41.0	30.0	
Physical properties						
Liquid limit, %	76.6	64.6	44.0	35.5	51.0	87.0
Plastic limit, %	25.6	17.6	21.1	17.5	25.5	52.2
Plasticity index	50.0	47.0	22.9	18.0	25.5	34.8
Chemical properties						
pH	7.1	8.2	8.4		5.7	
C.E.C.(soil passing No. 10 sieve, m.e/100gm)		27.5	14.5		8.4	
C.E.C.(soil passing No. 40 sieve, m.e./100gm)	41.0	33.1	13.4		13.5	
C.E.C.(soil passing No. 325 sieve, m.e./100gm)						
Carbonates, %	.8	16.1	7.2		0.1	
Organic matter, %	.2	0.1	0.6		0.1	
Predominant clay mineral[b]	M	M	I&C	I&C	K	M
Classification						
Textural[c]	Clay	Clay	Clay	Clay	Clay	Clay
Unified	CH	CH	CL	CL	CH-CL	CH
BPR(AASHO)	A-7-6(20)	A-7-6(20)	A-6-6(14)	A-6-(11)	A-7-6(11)	A-7-6(20)

[a]Textural gradation tests were performed only on the soil fraction passing the No. 10 sieve. All soils used contained less than 5% gravel.

[b]Symbols are M-montmorillonite, I-illite, C-chlorite, and K-kaolinite. Determinations were made by x-ray diffraction analysis.

[c]U.S.D.A. textural classification was used.

Table 3. Chemical composition of lime

Chemical constituent	Maximum amount present, % by weight
Ammonium hydroxide, ppt	0.60
Chloride	0.005
Heavy metals (as Pb)	0.003
Insoluble in HCl	0.05
Iron	0.05
Magnesium and alkali salts (as sulfates)	2.0
Sulfate	0.40
Minimum calcium hydroxide present	96.892

Fly Ash

Fly ash is the finely divided residue that results from the combustion of ground or powdered coal and is transported from the boiler by flue gasses. The fly ash used in this study was collected by a Cottrell precipitator at the St. Clair power plant of the Detroit Edison Co. in Detroit, Michigan. An analysis of this fly ash is given in Table 4.

Table 4. Composition and properties of St. Clair fly ash

Chemical constituent or property	Value with units as indicated
Silicon dioxide, % by wt.	41.9
Iron oxide, %	25.8
Aluminum oxide, %	22.5
Calcium oxide, %	2.7
Magnesium oxide, %	1.0
Sulfur trioxide, %	0.8
Available alkalis as sodium oxide, %	0.3
Loss on ignition, %	3.6
Specific gravity	2.61
Specific surface, sq cm/gm	2720
Retained on No. 325 sieve, %	11.3

Water

Throughout the laboratory work the water used for mixing of the specimens was distilled water obtained from an automatic water still. Distilled water was used to prevent carbonation of the lime by carbon dioxide in solution in ordinary tap water.

EQUIPMENT AND OPERATION

Optical

Binocular microscope

For general investigations of samples a Bausch and Lomb binocular microscope was used. This microscope has oculars of 10x and 15x powers and objectives of 0.66:1, 1.3:1, 3:1, and 6:1, thus allowing a maximum magnification of 90 times.

Petrographic microscope

Description. A Leitz research model petrographic microscope was used to determine the optical properties of the crystals.

Index of refraction. When light passes obliquely from one medium into another in which it travels with a different velocity, it undergoes an abrupt change in direction. This abrupt change in direction is known as refraction. The index of refraction is determined by the distance light will travel in a given time interval through a transparent substance as compared with air.

In practice the index of refraction of a crystal may be determined by the method of central illumination. The test is employed for comparing the crystal with various immersion media of known refractive indices in which they are mounted. Light enters from below and is transmitted through both media. At the bounding edge both reflection and refraction take place, and a portion of the entering beam is bent either to one side or to the other, depending upon the relative indices of refraction of the adjacent

media. If the two indices are the same, no refraction takes place. If they are not the same a portion of the beam will be deflected toward the mineral with the greater index. The deflection results in a light blur in the form of an irregular white line visible through the microscope just inside the boundary of the substance of greater index. If the tube of the microscope is raised an illusion is produced, the line appearing to move toward the substance of higher refractive index. If the two have the same index, no reflection or refraction can take place at the boundary between the two substances (23).

Interference figure. When convergent doubly polarized light is used to view a birefrigent crystal, it may be made to yield an interference figure. Minerals that have but one direction of isotropy produce a uniaxial figure which appears as an axial cross, whereas those with two such directions give a biaxial figure which is of the form of a right hyperbola or isogyre. Hexagonal and tetragonal crystals give an uniaxial figure whereas orthorhombic, monoclinic and triclinic crystals yield a biaxial figure. If a uniaxial crystal is mounted so that it is viewed in a direction coinciding with the optic axis (perpendicular to 0001) then the uniaxial cross will be centered in the field.

Optic sign. Doubly refracted rays of the uniaxial interference figure are arranged radially. The extraordinary ray vibrates in the principal plane parallel to the c-axis; the ordinary ray vibrates at right angles to this. If the ray vibrating in the principal plane is the slow ray of the crystal, the crystal is positive; if it is fast, it is negative. The position of the slow ray may be determined with a gypsum plate

inserted in the slot above the objective lens. In optically positive crystals subtraction occurs at right angles to the direction of the slow ray in the plate. In negative ones the subtraction is in the quadrants along the slow ray direction. This is recognized in the polarizing microscope by the appearance of a lens shaped blue color appearing in the quadrants containing the slow ray of the plate in the positive case and in the quadrants perpendicular to the direction of the slow ray in the negative case (23).

X-ray

Diffractometer

The diffractometer used was the General Electric XRD-5, a picture of which appears in Fig. 1A. Primarily this consists of a parafocussing x-ray diffraction apparatus which utilizes a geiger counter for directly measuring the intensity diffracted at any particular angle 2θ. From the Bragg equation,

$$n\lambda = 2d\sin\theta, \qquad 1$$

where λ = wave length of x-radiation,

the interplaner spacings, d, of the diffracting planes can be computed. By utilizing the diffractometer to determine the characteristic d-spacing and their intensities of an unknown or unknowns, the unknown in most cases can be determined by using the ASTM card file (3). This file lists the characteristic spacings and intensities for a large number of organic and inorganic compounds and can be rapidly utilized since they are sorted according to the Hanawalt grouping scheme.

Figure 1. X-ray equipment

A. Diffractometer
B. Powder camera
C. Weissenberg apparatus
D. Precession apparatus

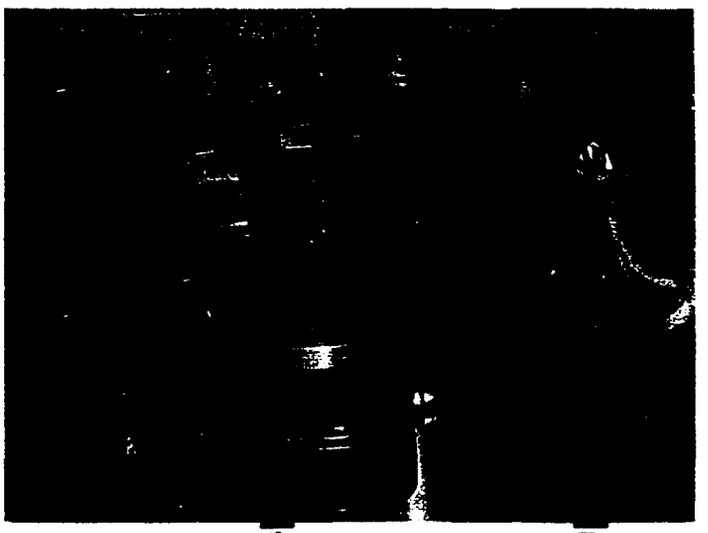

A B

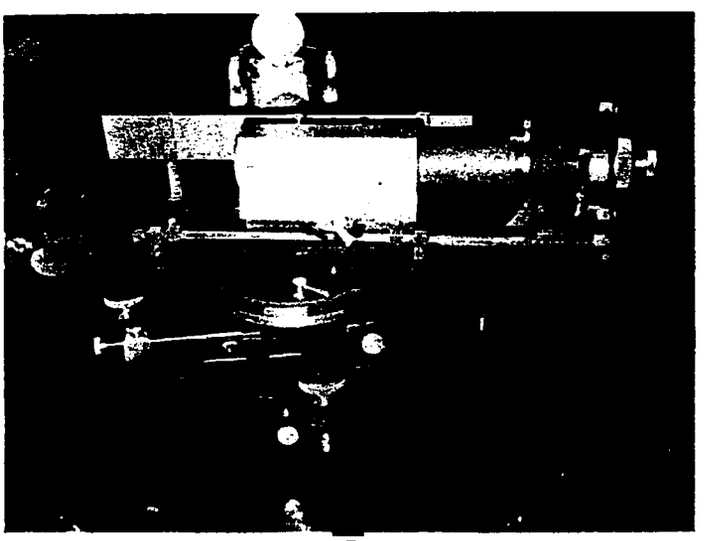

C

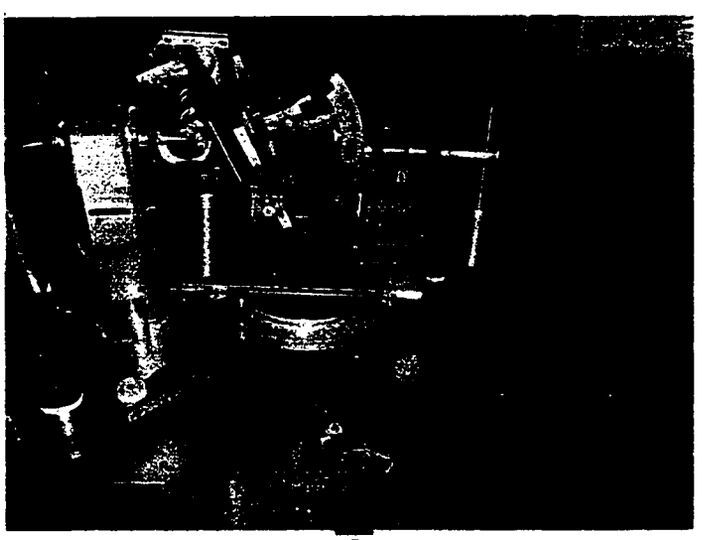

D

Debye-Scherrer Method

In this method a sample consisting of a crystalline powder is mounted in a cylindrical camera in such a way that the axis of the sample is parallel to the axis of the camera. A strip of photographic film is placed flush against the inner circumference of the camera. A collimator which limits the x-radiation to a narrow beam just wide enough to cover the sample is placed on the diameter line of the cylindrical camera and the sample is centered on this line. The sample is slowly rotated around its center while x-rays are passed through the collimator so that the diffraction diagram of the sample is recorded on the film. By employing a Straumanis film loading the points on the film making angles of 0 and 180° with the direct beam can be determined, the distance between them measured and from this the angle 2θ of any intermediate line can be accurately determined. The corresponding d-spacing can then be computed by the Bragg equation. The Debye-Scherrer camera used with the investigation conducted here is 57.5 mm in diameter and 70 mm in length (Fig. 1B). It is manufactured by Siemens and Halske Aktiengesellschaft, Karlsruhe, Germany, and is distributed in the U. S. by R. C. A. A film measuring device distributed by the same company permits a direct reading linear measurement of $\pm$.01 mm.

Rotating crystal method

The Weisenberg camera (discussed below) or the cylindrical camera discussed above can be used to take rotation x-ray pictures of a single crystal by aligning the rotating stage of the camera to 0°. In this method a single crystal is mounted on a short fiber of glass wool approximately along one of the crystal's axes. The fiber, in turn, is attached to a thin

glass rod. This rod is inserted into the head of a two circle goniometer and the crystal is aligned optically so that it will rotate about an axis. When the crystal has been aligned optically with as much precision as possible, the goniometer is placed on the rotating spindle of the camera. The crystal can then be brought into exact alignment by taking two oscillation photographs at 90° with each other and observing the position of points lying on the 0 layer line. The x-ray beam will then pass through the crystal perpendicular to the axis about which the crystal is rotating.

As the crystal rotates, the reciprocal lattice of the crystal accompanies it. Those reciprocal lattice points within range will pass through the sphere of reflection and, as each point cuts the sphere, a diffracted beam will be developed.

The diffracted rays are recorded on a cylindrical film whose axis is parallel and concentric with the rotation axes. The spots on the film produced by the diffracted rays will produce a two dimensional pattern following the geometry of a Bernal chart. For comparison with an actual rotation picture see Figure 4, p. 38.

The straight lines in the y or ζ direction

$$\zeta = \frac{y}{r^2+y^2} \qquad 2$$

are called layer lines of the first kind or simply layer lines and are lines of constant ζ value; those in the x or ξ direction

$$\xi = \sqrt{\left[1+\frac{r^2}{r^2+y^2} - \frac{2r}{(r^2+y^2)}\,\mathrm{Cos}\,\frac{(180x)}{(\pi r)}\right]} \qquad 3$$

are layer lines of the second kind or row lines. The layer lines lie on the circumference of the cylindrical film and the row lines along the axial length of the film. If a hexagonal crystal is rotated about its c-axis,

all spots lying on the same layer line will have the same ℓ index and those lying on any one row line will have the same hk index.

The Bragg angle θ may be found by superimposing the Bernal chart over the film, reading the value of ξ and ζ for each spot, and using the relation

$$\xi + \zeta = d^{*2} = 4\mathrm{Sin}^2\theta \qquad 4$$

where d^* = interplanar dist. in reciprocal lattice.

Or θ may be found by measuring the x and y coordinates of each spot on the film and using the relationship that

$$\mathrm{Cos}\ 2\theta = \mathrm{Cos}\,\tau\ \mathrm{Cos}\,\chi \qquad 5$$

where $\tau = 2x$

and $\chi = \mathrm{Tan}^{-1}\frac{2y}{D}$

and D = camera diameter in mm.

Weissenberg Method

The rotating crystal method has several rather serious limitations. A superposition of several reflections occurs causing difficulty in unequivocally indexing the reflections and determining their intensities.

One method to resolve individual reflections is to displace the film after one reflection has been recorded so that no two reflections strike the film in the same place. The Weissenberg method accomplishes this by translating the film in a direction parallel to the rotation axis at a rate, $\not\equiv$, proportional to the angular rotation of the crystal, ω . To give undistorted scale photographs $\frac{W}{Z} = 2\ \frac{\text{Degrees}}{\text{mm.}}$ or for every two degrees the crystal rotates the film should be translated one millimeter. In order to permit only one layer line at a time to be recorded, the diffraction cone of this

layer must be isolated. To accomplish this the crystal is covered with a closed hollow metal cylinder and the desired layer line cone is singled out by permitting it alone to emerge from the cylinder through a circular slit. The particular layer line desired is selected by moving the cylinder an appropriate amount (s) to permit the desired cone to pass through the slit. The amount of translation required is given by

$$S = r \tan \nu_n \qquad 6$$

where r = film radius

and $\tan \nu_n = \frac{Yn}{r}$.

Several different types of Weissenberg methods are possible but in this study only the equi-inclination Weissenberg method was utilized since photographs taken by this method are much more easily interpreted than by the other methods. In this method the beam is inclined at an angle $\mu = -\nu$ where ν is equal to the relationship given above or more conveniently by

$$\nu = \text{Sin}^{-1} \frac{\rho}{2}. \qquad 7$$

Conveniently, Buerger (5) presents charts on pp. 294 and 295 giving the angle μ in terms of the reciprocal lattice level coordinate, ρ , or the height, y, of the layer line for a 57.3mm camera diameter. Also he gives a graph for the determination of the layer line screen settings, s, in terms of μ .

In the equi-inclination method any central layer line projects on an n-level Weissenberg photograph as a straight line of slope 2 since this method brings the crystal rotation axis exactly on the circumference of the reflecting circle. By a central lattice line is meant a line connecting reciprocal lattice points one of whose indices in planes perpendicular to

the rotation axis is zero. Thus for a reciprocal lattice plane perpendicular to an n-fold axis there will appear on an equi-inclination Weissenberg photo central lattice lines at a period $\frac{360^{o}}{n}$. Non central lattice lines will project as ovals, the ovals assuming the same geometric pattern for each level. By combining two of these patterns separated 90^{o} from each other, a template may be constructed permitting indexing of the reflections directly.

On the basis of the intensity, the symmetry, and the period displayed by the reflections on the Weissenberg photograph, the plane point group and the centro-symmetrical crystal class is determined. On the basis of the above plus the systemmatic absences of characteristic reflections, a diffraction symbol can be assigned to the information gleaned from the crystal and the space group may be determined unequivocally in some cases and, in others, at least narrowed down to the choice of two or three alternative ones. Unfortunately x-ray photographs of crystals always cause the crystals to appear to be centrosymmetrical; thus, in some cases, the space group is not uniquely determined. In these cases methods other than x-ray must be employed to finally determine the space group.

The Weissenberg apparatus used in this study was manufactured by Otto von der Heyde Co. in Newton Highland, Mass. and a picture of the apparatus appears in Figure 1C.

Precession method

In the precession method the reciprocal lattice of a crystal is recorded without any distortion. Because of this feature a simple inspection of the film is sufficient to determine the symmetry of the layer being

photographed and the indices of each reflection present on the photograph. In order to record the reciprocal lattice, a rational direction of the crystal is caused to take a precessing motion, the crystal being supported at the unmoved point of a universal joint. In order to provide an undistorted registry of the reciprocal lattice on the film, the film must also follow the identical precessing motion of the reciprocal lattice plane being photographed, remaining always parallel to it.

The diffraction corresponding to a single layer of the reciprocal lattice must be isolated for each photograph. Since the locus of diffraction directions for a single layer is the surface of a circular cone, this cone can be isolated by permitting it to pass through an annular aperture in a flat screen which is placed between the crystal and the film. The proper distance, s, of the layer line screen from the crystal to isolate a particular diffraction cone is given by

$$s = r_s \cot \cos^{-1}(\mathrm{Cos}\,\bar{\mu} - d^*)$$

where r_s = radius of annular aperture

and $\bar{\mu}$ = precession angle

and d^* = spacing of reciprocal lattice planes.

To determine lattice constants from the 0-level precession photograph it is only necessary to measure the distance, x, on the film which is the distance between two applicable reference points. Since the distance, x, on the film is directly proportional to the corresponding reciprocal lattice distance x of the crystal, then $x^1 = Fx$ or

$$x = \frac{1}{F} x^1$$

where F = proportionality constant equal to dist. from crystal to film.

The translation, t, in the direct lattice is then

$$t = \frac{n\lambda}{nd^*} \qquad 10$$

where nd^* = dist. x of eq. 9

and n = no. of lattice rows between which dist. x^1 was measured

and λ = wave length of radiation used (4).

The apparatus used in this work was manufactured by the Charles Supper Co. of Newton Center, Massachusetts, and a picture of the apparatus appears in Figure 1D.

Differential Thermal Analysis

The method of differential thermal analysis involves the use of a test specimen and a neutral body, usually a powder which has no transformation and whose thermal properties approximate those of the test specimen. The neutral body is used as a comparison standard. The specimen and the standard are heated simultaneously at the same rate through the same temperature interval. A differential thermocouple whose two junctions are located in the specimen and in the standard will remain at zero total limit as long as no thermal reaction occurs. When the specimen being tested undergoes a transformation, the heat effect creates a difference in temperature between the specimen and the comparison standard. This difference in temperature is registered by the recorder on graph paper as well as the temperature at which the reaction occurs. From this data certain qualitative and quantitative determinations can be made.

The apparatus used was constructed by personnel in the Iowa Engineering

Experiment Station Soil Research Laboratory; the controls were manufactured by the Minneapolis-Honeywell Corporation.

MIXTURE PREPARATIONS AND INVESTIGATIONS

Preliminary Work

As mentioned in the introduction, the first indication of the presence of reaction products was found on subjecting to x-ray diffractometer analysis mixtures of soil M-67, 12% lime, and water (above the liquid limit), which had been prepared for the determination of liquid limits. The results of this analysis showed new x-ray "peaks" occurring at 8.11 and 7.60 Angstroms (11). However, in 2 inch x 2 inch specimens compacted at optimum moisture content no such peaks were observable.

Petrographic microscope examinations of the liquid limit mixtures were attempted to isolate the reaction products formed, but no new substances were observed. It then became the object of this phase of the research to attempt to grow euhedral crystals of these reaction products of at least microscopic size and to determine their properties. To accomplish this various phase relationships were investigated empirically in order to attempt to produce recognizable crystals.

Trial Mixtures

Lime-water-soil systems

Water as the variable parameter. That the clay fraction of soil M-67 was the actively participating part of the soil in the reaction with lime appeared to be a reasonable assumption. Therefore soil M-67 was shaken through a 325 mesh sieve to obtain the finest fraction of the soil possible through purely mechanical separation. In order to obtain the most

representative sample possible the sieve pan was emptied often and the material remaining on the 325 sieve was continually repulverized. This process was repeated until only a negligible amount of soil passed through the sieve during a thirty minute period. Washing the material through the sieve was not attempted in order to avoid any process which might change the nature of the clay before being mixed with lime.

This material was then mixed with 20% lime by weight of oven dry soil, and distilled water was added in amounts of 110, 100, 90, 80, 70, 60, 50, 40, 30, and 20% by dry weight of soil plus lime. The materials were mixed in polyethylene plastic containers. After thorough mixing the containers were covered with snap type lids and placed in a controlled temperature-humidity room (70°F and 95% relative humidity).

After thirty days the containers were removed and a sample of the mixture from each was subjected to x-ray diffractometer test, the results of which appear in Figure 2. Since the mixtures were smoothed into the sample holders by longitudinal strokes with a glass slide, preferred orientation of the particles was attained. From the diffractometer traces it is evident that the reaction products were present in greater quantities at high moisture contents. At moisture contents below 40% the product peaks almost disappear, which explains why specimens compacted at optimum moisture give no indication of these reaction products when subjected to x-ray analysis.

Two reaction product peaks are evident in Figure 2. The one at 8.11 Å is probably the second order basal reflection from montmorillonite, sharpened considerably by the action of adsorbed calcium and reaching maximum height at higher moisture contents. The 7.59 Å peak is that of a

Figure 2. Diffractometer charts, Cu Kx radiation mixtures of soil M-67, lime, and variable water after curing for 30 days

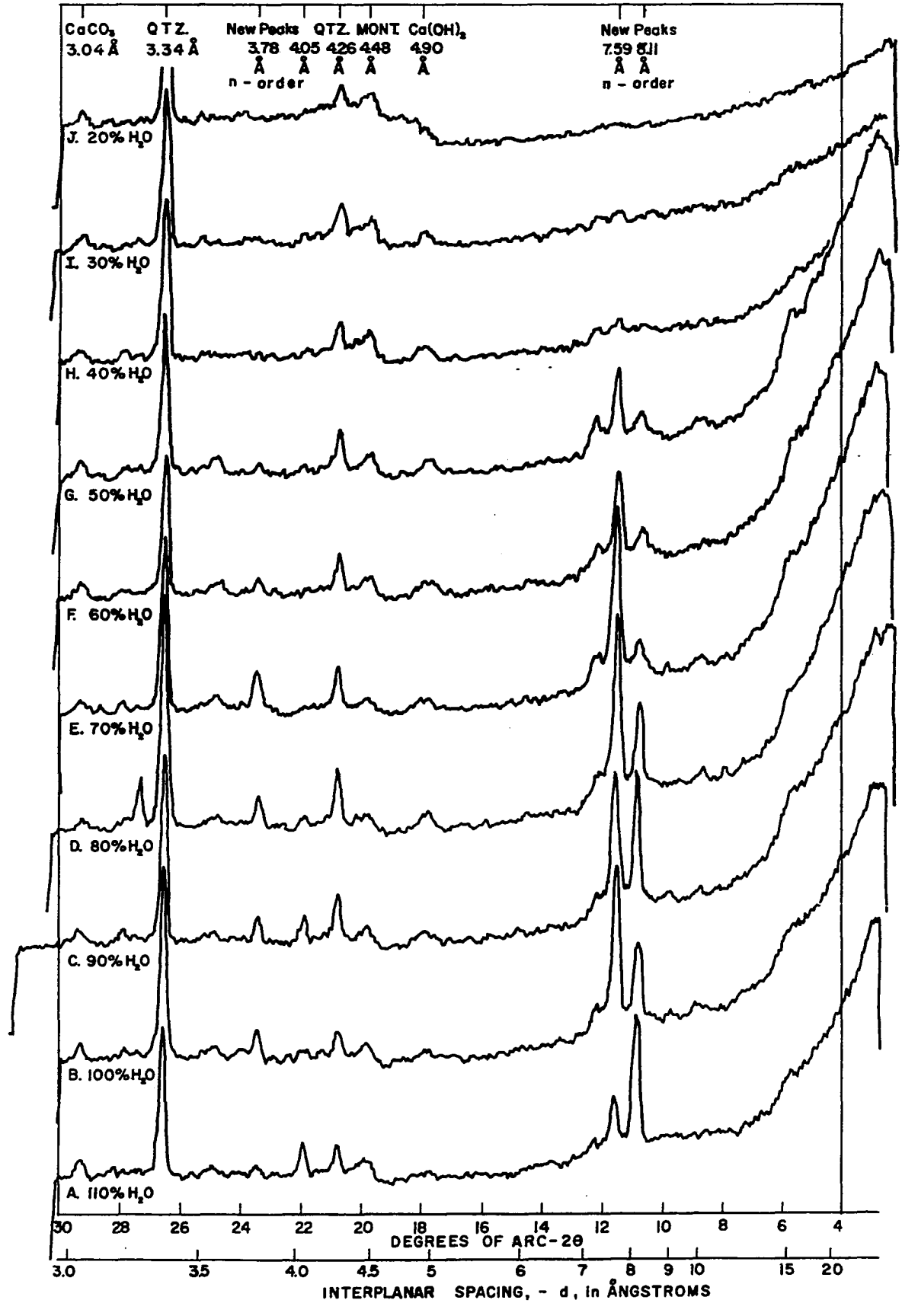
CaCO3 3.04 Å
QTZ. 3.34 Å
New Peaks 3.78 Å 4.05 Å 4.26 Å
QTZ. MONT 4.48 Å
Ca(OH)2 4.90 Å
n - order
New Peaks 7.59 Å 8.11 Å
n - order
J. 20% H2O
I. 30% H2O
H. 40% H2O
G. 50% H2O
F. 60% H2O
E. 70% H2O
D. 80% H2O
C. 90% H2O
B. 100% H2O
A. 110% H2O
30 28 26 24 22 20 18 16 14 12 10 8 6 4
DEGREES OF ARC-2θ
3.0 3.5 4.0 4.5 5 6 7 8 9 10 15 20
INTERPLANAR SPACING, - d, in ÅNGSTROMS

crystalline reaction product and will be discussed in more detail later.

Optical examination of the mixtures under the binocular and petrographic microscopes disclosed the formation of euhedral crystals of hexagonal shape. Although these crystals were quite small, the larger ones being of the order of 50 μ across the flats by 5 μ thick, x-ray powder photographs of minute amounts showed them to be the crystals being sought, corresponding to the 7.59 Å peak of Figure 2.

Soil M-67 passing the 270 mesh sieve and retained on the 325 mesh sieve, 20% lime, and 100% water were mixed, cured for thirty days, and subjected to x-ray diffractometer analysis. No new peaks were formed confirming that it was the clay fraction of the soil entering into the reaction.

From the variable water investigation it appeared that it would be advantageous to mix the samples at high moisture contents and this was done with the mixtures prepared later.

Lime as the variable parameter. Using the relation that mixtures should be of high moisture content, the effect of varying the amounts of lime was investigated at a constant moisture content of 105%. Lime was mixed with soil M-67 in quantities of 5, 10, 15, 20, 25, 30, and 50% by weight of dry soil. X-ray diffractometer traces were run on these mixtures after 30 days moist curing. It was found that the height of the new peaks grew successively larger as the percentage of lime was increased to 20%, and above this the height remained relatively constant while the height of the residual calcium hydroxide peak increased. Thus it appeared that for a thirty day period the optimum lime content was about 20% for this soil.

Under the microscope, the same extremely small euhedral crystals were observed scattered through the matrix in those samples containing 10% lime or more.

Soil as the variable parameter. Other soils were also investigated as to their reaction with lime. These soils included M-51, IC-44, IC-41 and K-30. Of these only the montmorillonite soil M-51 showed any significant height of new peaks. Soil K-30 gave a slight indication and the others none at all. However, these mixtures were allowed to cure for only 30 days. As will be seen later, it would be advantageous to let them cure for six months and then examine them by x-ray diffraction.

Lime-water-bentonite investigation

Since the main component in soil M-67 is montmorillonite clay, and since it is the clay fraction which is reacting with the lime, it appeared logical that better results might be obtained by mixing a bentonite with lime. For this purpose, a bentonite from Otay, California, was selected because of the low amount of impurities it contains (13). Since the amount of montmorillonite was increased, the amount of lime added was also increased to 40% by dry weight of bentonite. Water was added in the amount of 110% by dry weight of bentonite plus lime. Several samples were made and one was tested after 30 days moist curing. The results of the x-ray analysis on this sample were disappointing in that only a small peak appeared at the expected interplanar spacing and no crystals could be located with the microscope. The other samples were allowed to remain in the humidity room for seven months before being tested.

When, after seven months, they were examined under the microscope,

crystals which were large in comparison with those obtained previously were found in comparative abundance. The larger ones were about 500 μ across the flats by 20 μ thick. From these the size graded down to submicroscopic. The crystals occurred singly, generally with the basal plane oriented in a vertical direction; in clusters of two or three apparently twinned; or in clusters containing scores of individual crystals in random orientations. A microscopic photograph of these crystals appears in Figure 3, A. Since crystal formation was so much more rapid in soil M-67 than in the bentonite, the soil montmorillonite must be either less well crystallized or else the soil must contain ions which act as accelerators for the reaction.

Lime-water-fly ash investigation

Since fly ash is well known for its pozzolanic properties and since it has been used with lime in soil stabilization, a mixture of fly ash plus 30% lime plus 100% water was mixed and placed in the humidity room. After seven months curing it was removed and investigated under the microscope. Large euhedral crystals had been formed throughout the mixture with similar geometric properties to those from the bentonite. A microscopic photograph of these crystals is reproduced in Figure 3, B.

The 7.59 $\mathring{A}$ basal spacing was observed, but a powder photograph was not made for several months. After several months, a powder x-ray analysis by Dr. R. H. Handy, Assoc. Professor of Civil Engineering, showed that the substance had become amorphous, whereas those crystals produced from bentonite retained their crystallinity.

By the heavy liquid method, the specific gravity was determined to be

Figure 3. Microscopic photographs of reaction product crystals

1.98 $\pm$ .01. By the method of central illumination, the index of refraction of the ordinary ray (W) was found to be 1.543 $\pm$ .002.

RESULTS

Optical Properties

Crystal selection

Under the binocular microscope a search was made for several of the largest perfect single crystals in the bentonite sample. These crystals were carefully removed from the matrix and placed on a glass slide. Here they were cleaned of all adhering fragments by means of a single hair. They were then transferred to a second slide and a cover glass was placed over them for examination under the petrographic microscope. Doubly polarized light was used to determine which of the crystals selected were, in fact, perfect and free from inclusions, twinning, and intergrowths.

Index of refraction

Those crystals determined to be acceptable were transferred to individual slides for determination of the refractive index by the method of central illumination. The crystals were mounted in various immersion media of known refractive index and were examined under the microscope. A blue filter was inserted between the light source and the mirror to approximate a daylight source. Twenty crystals were examined and all had a refractive index greater than 1.545 but less than or equal to 1.550, thereby establishing the index of refraction of the ordinary ray (perpendicular to 0001) of $1.548 \pm .002$. Because of the extreme thinness of the crystals, the refractive index perpendicular to this direction (extraordinary ray) was not determined exactly; however, it was considerably less.

Interference figure and optic sign

A crystal mounted on a slide with the basal pinacoid (0001) perpendicular to the axis of the scope was viewed under convergent doubly polarized light with the Bertrand lens inserted. An axial cross appeared in the field with no movement of the isogyres apparent when the stage was rotated. On insertion of a gypsum plate in the slot above the objective, a lens shaped blue color appeared in the quadrants perpendicular to the direction of the slow ray in the plate thus determining the crystal to be uniaxial negative.

Physical Properties

Geometry

In plane polarized light the crystals were transparent and colorless, platelike, and hexagonally shaped with beveling observed on the edges. A measurement of the hexagonal interior angles showed them to be exactly 60°.

Specific gravity

The heavy liquid method was used to determine the specific gravity of the crystals. In this method the crystal is immersed in a liquid of known density. If the crystal is denser than the liquid it will sink to the bottom; if less dense it will float. At some density of the liquid the crystal will neither sink nor float but will be suspended in the liquid. The density of the liquid and the crystal are then the same.

In this study, mixtures of bromoform (g = 2.890 @ 20°C) and carbon tetrachloride (g = 1.595 @ 20°C) were varied to bracket the density of the

crystal. Near the density of the crystals the mixture was varied in intervals of 0.005 gm/ml. A 5 ml sample was removed by a pipette at each point and weighed on an analytical balance to determine the exact density of the mixture. All of the crystals sank to the bottom at a liquid density of 2.060 and all were floating at 2.080 gm/ml; at intermediate densities crystals were observed in all three positions, floating, suspended, and on the bottom, establishing the specific gravity of the crystals at 2.07 ± 0.01.

X-ray Investigations

Rotating crystal cylindrical camera

A single crystal free from inclusions was mounted on a short fiber of glass wool with Duco cement thinned with amyl acetate so that the c-axis was the axis of rotation. The crystal was first aligned optically by means of a single crystal orienter and then was brought into exact alignment by oscillating x-ray photographs taken at ninety degrees with each other.

After alignment was completed, a fifteen hour 360° rotation exposure was made. A print from this film is shown in Figure 4 from which the d-spacings and intensities for all spots observed on the film are tabulated in columns 1 and 2 of Table 5. Because of the size of the spots and since film shrinkage cannot be computed, the accuracy of these d-spacings is not so good as can be obtained by some of the other methods. However, a great deal of useful information can be obtained from this method in conjunction with the Weissenberg method.

Figure 4. Single crystal rotation photograph of reaction product crystal, Cu K_d radiation

Table 5. Diffraction data, Cu K_{α} radiation.

Single x-tal rotation		Hex.[a]	Rhom.	Powder camera[b]		Back Refl. Weissenberg
d	I	hk·l	hkl	d	I	d
7.75	10	006	222	7.59	10	
3.83	7	018	332	3.85	7	
3.83	5	0012	444			
3.44	4	1010	433	3.42	4	
2.90	8	110	101	2.87	9	
2.86	1	113	210			
2.72	4	116	321	2.71	1	
2.54	6	1016	655	2.52	6	
2.54	8	119	432			
2.50	1	202	200	---		
2.46	7	024	220	---		
2.34	9	1112	543	2.33	6	
2.31	6	208	422	2.30	8	
2.22	6	0210	442	2.20	4	
2.14	10	0120	776	2.11	5	
2.13	5	1115	654			
2.08	1	1211	542	---		
2.01	6	2014	644	2.07	1	
1.96	1	1022	877	---		
1.94	5	1118	765	1.93	3	
1.92	4	0216	664			
1.88	4	214	310	1.86	3	
1.87	4	125	320			
1.81	3	128	431	1.79	1	
1.76	1	2110	532	---		
1.73	1	2122	976	---		
1.71	9	2020	866	1.72	4	
1.69	3	2113	655	---		
1.68	9	300	112	1.66	5	1.706
1.66	2	1214	653			
1.64	1	1124	987	1.63	4	
1.64	7	306	411			
1.594	3	2116	754	----		

[a]Other hexagonal indices observed on Weissenberg photographs in addition to the one listed, x0z, when $z \neq 3n$, are xxz, 0xz, 0xz, x0z, and xxz. Other indices observed in addition to 0yz when $z \neq 3n$ are y0z, yyz, y0z, yyz, and 0yz. Other indices observed in addition to xyz when $z \neq 3n$ are x,x+y,z; x+y,x,z; y,x,z; y,x+y,z; x+y,y,z; y,x,z; y,x+y,z; x+y,y,z; x,y,z; x,x+y,z; x+y,x,z. All possible indices observed when z = 3n.

[b]In addition to the powder camera data indicated in the table, lines were also observed at 8.29, 5.52, 4.45, and 3.16 Angstroms which were identified as montmorillonite.

Table 5. (continued)

Single x-tal rotation		Hex.	Rhom.	Powder camera		Back Refl. Weissenberg
d	I	hk·l	hkl	d	I	d
1.54	5	3012	633	1.53	3	
1.483	6	1220	875	1.475	4	
1.464	3	2026	1088	----		
1.45	6	220	202	1.438	1	1.465
1.43	4	226	420	1.416	1	
1.396	2	131	242	-----		
1.38	1	315	410	----		
1.36	4	2212	642	1.355	2	
1.301	3	1226	1097	1.303	2	
1.279	1	1316	763	----		
1.229	1	048	440			
1.200	2	3120	965	1.195	1	
1.166		1322	985	1.166	1	
1.131	1	238	530	1.137	1	
1.121	2	3210	731	----		
1.109	1	0420	884	---		
1.097	5	410	213	1.089	1	1.094
1.092	3	2314	752			
1.088	3	416	510	1.081	1	
1.072	1	3216	870	-----		
1.056	4	4112	732	1.050	1	
1.034	3	2320	974	1.029	1	
0.984	1	0510	810	---		
0.967	3	330	303	---		0.963
0.960	1	5014	833	---		
0.958	2	336	521	---		
0.937	1	3312	741	0.933	1	
0.926	2	324	411	---		
0.923	2	5020	1055	---		
0.876	2	4220	1064	---		
0.843	2	606	600	---		
0.841	2	1520	983	---		
0.836	2	600	224	---		0.8314
0.818	2	5212	831	---		
0.803	5	520	314			0.7988

Indexing of reflections

Weissenberg photographs were taken of each layer line from 0 to 26 which was observed in the single crystal rotation photographs. Prints of the zero level and the twentieth level appear in Figures 5 and 6. Each of the twenty-six levels were indexed by means of the template discussed earlier and the results are tabulated in column 3 of Table 5.

Since the central layer lines occurred at sixty degree intervals, the crystal system was confirmed as being hexagonal. By noting the Weissenberg projections of chains of diamond-shaped cells along the position-symmetry lines when $l = 3n$ and when $l \neq 3n$, it is apparent that the point of the diamond is displaced from the origin when $l \neq 3n$ which uniquely characterizes the rhombohedral division of the hexagonal system.

A characteristic of the single crystal rotation photograph is that for rotation about the c-axis all spots in any row line will have the same combination of hk indices, which serves as a check on the Weissenberg indexing. Table 6 lists the characteristic hk indices for each row line observed on the film in Figure 4.

To convert the hexagonal indices given in column 3 of Table 5 to rhombohedral indices, the relationships given by equations 11, 12, and 13 were used.

$$h_R = 1/3\ (2h + k + 1) \qquad 11$$

$$k_R = 1/3\ (-h + k + 1) \qquad 12$$

$$l_R = 1/3\ (-h - 2k + 1) \qquad 13$$

The results of this conversion appear in column 4 of Table 5.

Figure 5. Zero level Weissenberg photograph of reaction product crystal, Cu radiation

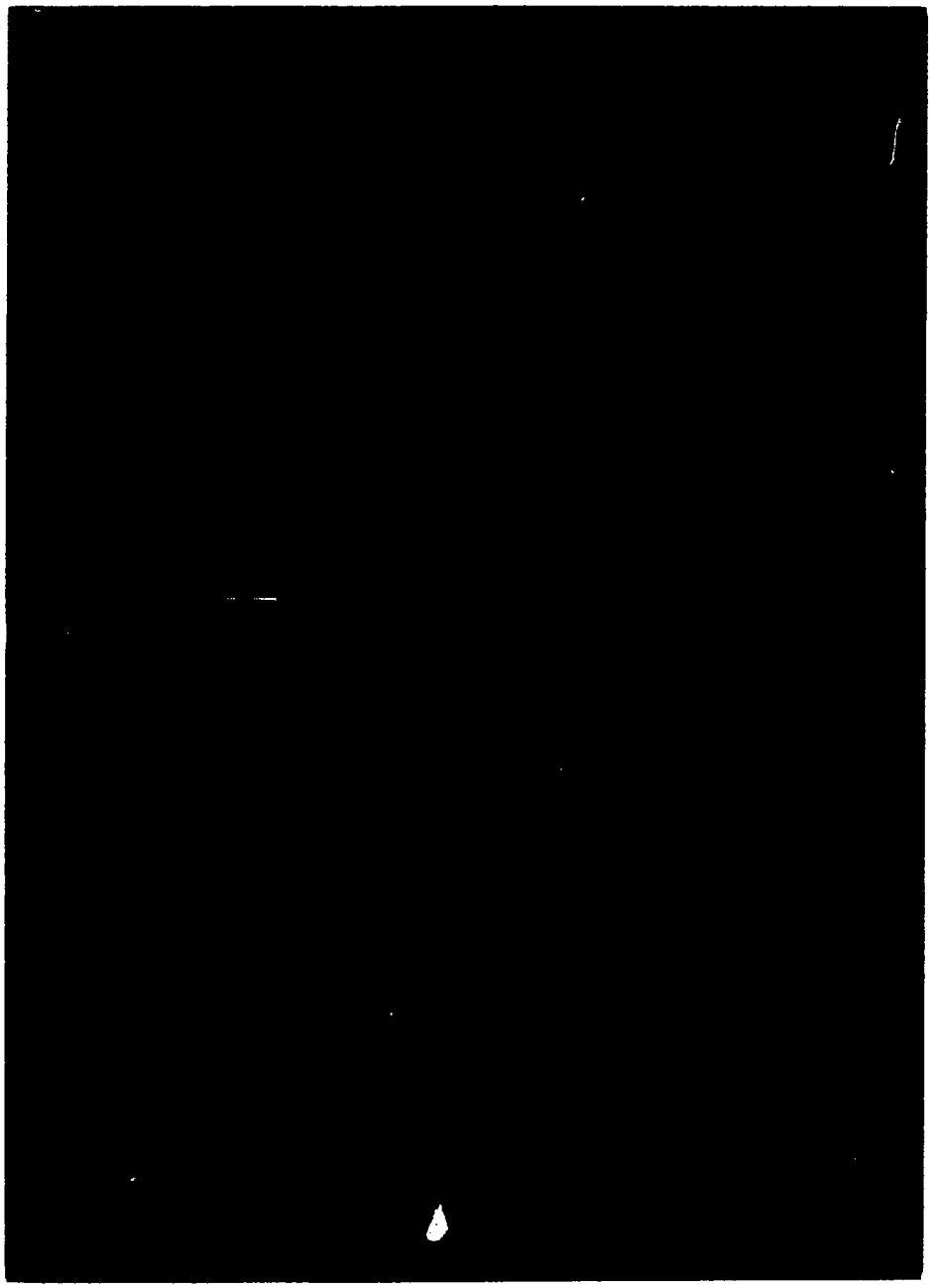

Figure 6. Twentieth level Weissenberg photograph of reaction product crystal, Cu radiation

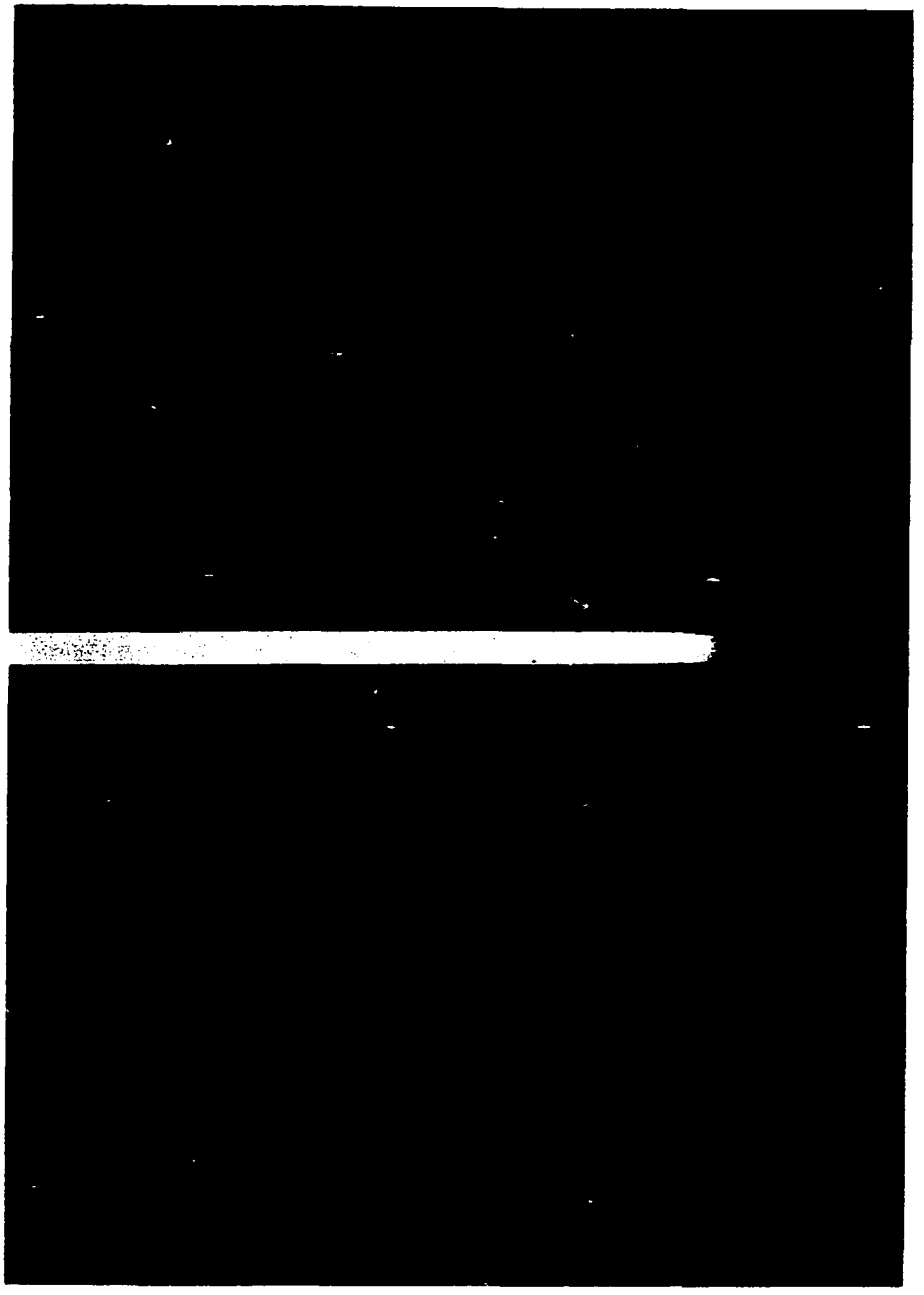

Table 6. Row line indices

Row line	hk	h + k
1	1,0	1
2	1,1	2
3	2,0	2
4	2,1	3
5	3,0	3
6	2,2	4
7	1,3	4
8	4,0	4
9	3,2	5
10	4,1	5
11	5,0	5
12	3,3	6
13	4,2	6
14	1,5	6
15	6,0	6
16	5,2	7

Hexagonal lattice constants

The powder camera film taken with copper radiation unfortunately had few lines in the back-reflection region. Therefore, to move more of the lines into the back-reflection region, chromium radiation was used. With more lines in the back-reflection region, film shrinkage can be precisely computed which eliminates the shrinkage error in the lattice constants determinations.

A fine collimator (0.7 mm) was used with a helium atmosphere about the crystal to decrease air absorption and scattering with this weaker

radiation. Temperature during the 1 hour exposure was maintained at 29° C. A Straumanis film loading was used and a print from this film is shown in Figure 7.

The a_0 and c_0 constants were computed from the measured d-spacings corrected for film shrinkage and were extrapolated against the function

$$\frac{\text{Cos}^2\,\theta}{\text{Sin}\,\theta} + \frac{\text{Cos}^2\,\theta}{\theta} . \qquad 14$$

Table 7 gives the a_0 and c_0 constants for the reflections listed which represent results of the ninth a/c approximation and recalculation. Since there was no slope to the θ plot, the average value of the computed constants may be used.

Table 7. Hexagonal lattice constants, Cr K_α radiation

hkl	a_0	hkl	c_0
30·0	5.7549	20·20	46.659
22·0	5.7552	21·16	46.689
22·6	5.7549	30·12	46.657
	Av. 5.7550	12·20	46.611
		20·26	46.687
		12·26	46.640
		31·20	46.663
	a/c = 0.12335		46.627
			Av. 46.654

The standard deviation of the above values is 0.025 which gives 90% confidence limits for c_0 of 46.654 ± 0.018.

A further check on the a_0 lattice constant was made by the back reflection Weissenberg method, data for which appear in column 8 of Table 5. Extrapolation of this data against the θ-function, equation 14, gives an

Figure 7. Powder camera photograph of reaction product crystal, Cr K_{α} radiation

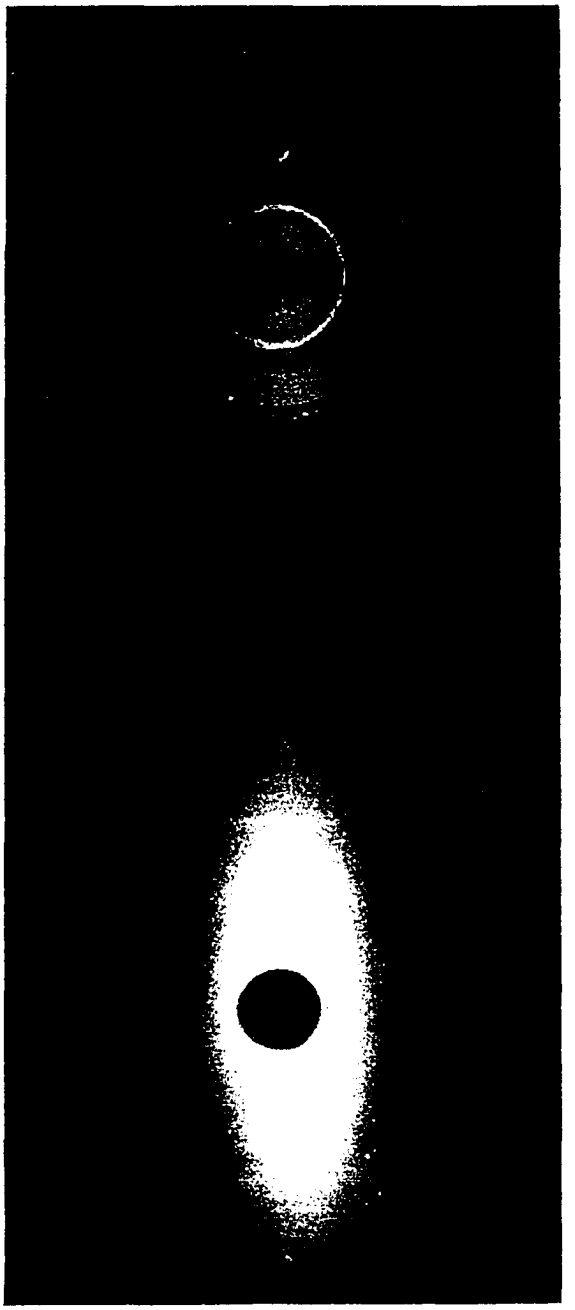

a_0 = 5.756 Å. Since the line breadth on the powder camera film is finer than that of the spots on the Weissenberg film, more accurate determinations are possible utilizing the powder camera.

A rough check on the c_0 spacing is possible by utilizing the single crystal rotation photograph. The layer line spacing, ζ, of the reciprocal lattice is given by equation 2. To find the identity period along the rotation axis (c) of the crystal, equation 15 is used.

$$c_0 = \frac{n\lambda}{\zeta_n} \qquad 15$$

The average of the ζ's for the first sixteen layer lines was used and a value for c_0 of 46.72 Å was computed. Since film shrinkage could not be computed for this film the c_0 spacing compares favorably with that shown in Table 7.

Hexagonal cell volume

The volume of the hexagonal unit cell is given by

$$V = \tfrac{1}{2}\sqrt{3}\, a^2\, c. \qquad 16$$

Since a_0 = 5.7550 Å and c_0 = 46.654 Å, then the volume is 1338.17 $Å^3$ or $133.817 \cdot 10^{-23}$ cm^3.

Rhombohedral cell lattice constants

Designating the hexagonal lattice constants as a_H and c_H, the corresponding rhombohedral constants are

$$a_R = 1/3\sqrt{3a_H^2 + c_H^2} \qquad 17$$

$$\sin\frac{\alpha}{2} = \frac{3a_H}{2\sqrt{3a_H^2 + c_H^2}} \qquad 18$$

and a_R = 15.902 Å and α = 20.850°. The shape of the rhombohedral unit cell is shown in Figure 8.

Thermal effect on lattice constants

A number of crystals were preferentially oriented on a slide in such a manner that only 00.ℓ indices would be recorded by the diffractometer. After heating the crystals for one hour at 110° C a small reduction in the c_0 lattice constant was observed with no loss in intensity or sharpness of the peak, which reduction is attributed to loss of zeolitic water. After one hour at 200°C, no further shift in d-spacing was observed; however, the peak became broader and intensity decreased considerably indicating a partial breakdown of the crystal lattice attributable to a partial loss of bound water. At 300°C only a very broad halo remained at the position of the 00.6 reflection indicating complete collapse of the crystal structure through loss of the remaining bound water. However, even at higher temperatures the external form of the crystals remained unchanged.

Space group determination

It has already been shown (p. 42) that the crystal belongs to the rhombohedral division of the hexagonal system. Other information is also available from the Weissenberg photographs to help in the space group determination.

By comparing the zero level photograph of Figure 5 (and all other 3n levels) with Figure 236 in Buerger (5) it is apparent that these levels have the characteristic appearance of plane point group $C_{6\ell}$. On the

Figure 8. Geometry of rhombohedral unit cell of reaction product crystal

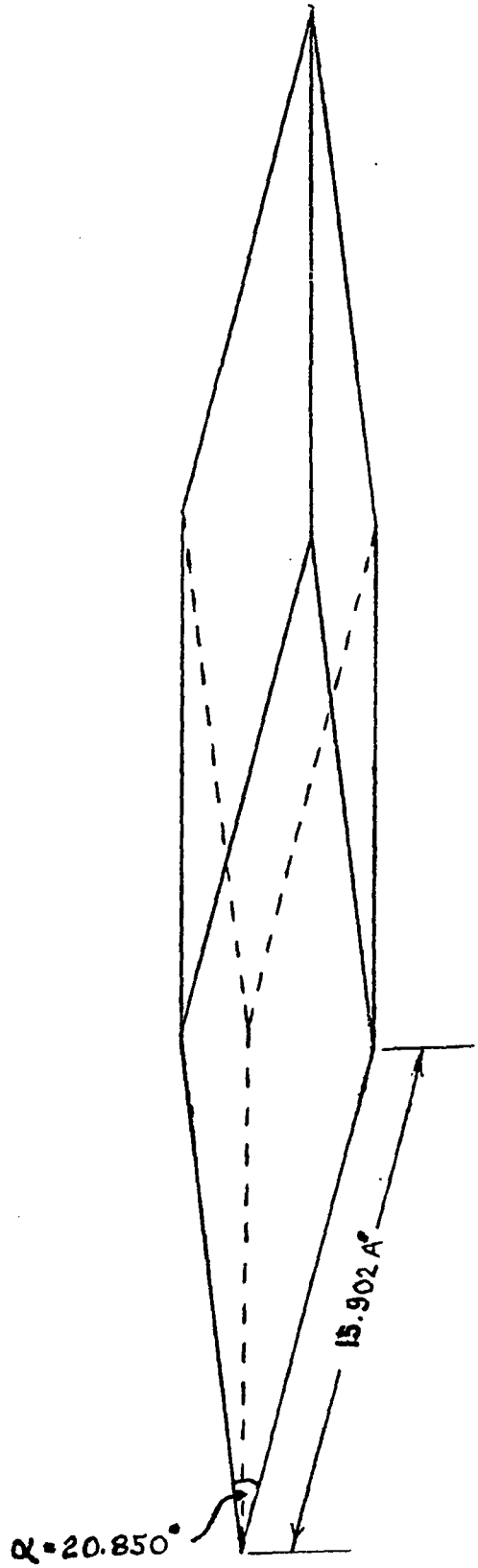
15.902 Å
α = 20.850°

original films even more so than on the prints, the intensities of spots at the same height about a central line can be seen to be equal. The films of all other levels (e.g. Figure 6) show the same relationship of the intensities; however, on levels other than 3n, the plane point group is $C_{3\ell}$ since the period is 120°. Table 28, p. 474, of Buerger (5) identifies this combination as belonging to centrosymmetrical crystal class D_{3d}.

With this information it is now possible to determine the possible space groups to which the crystal may belong by observing any systematic absences of reflections.

No systematic absences were observed in the general hkl reflections for the rhombohedral cell (Appendix 1, Table 8). In the hhℓ reflections, (Appendix 1, Table 12), the only ℓ indices occurring were for those in which ℓ = 2n indicating a (110) glide plane of component $\frac{c}{2}$ (c-glide). In the h00, 0k0 and 00ℓ reflections (Appendix 1, Table 14), h, k, and l, respectively, were equal to 2n indicating [100], [010], and [001] screw axes of components $\frac{a_1}{2}$, $\frac{a_2}{2}$, and $\frac{a_3}{2}$.

Unfortunately, x-ray photographs cannot distinguish between the presence or absence of a center of symmetry. Thus, although it is known that a three-fold axis is present, it is not possible to determine whether it is a rotation or an inversion axis.

Still, since it is known that the crystal has a three-fold axis, is rhombohedral, has a c-glide, and belongs to the centrosymmetrical class D_{3d}, the space group then must be either D_{3d}^6 ($R\bar{3}c$) or C_{3v}^6 (R3c). Of these two space groups D_{3d}^6 is the more probable since the number of general and

special positions for the ions are much more numerous in this group than in C_{3v}^6, thus better accommodating the somewhat complex molecules.

Chemical Properties

Solubility

The crystals are soluble in most dilute acids including sulfuric, acetic, and 0.05 normal hydrochloric acid.

Chemical analysis

The total amount of crystals separated during the course of this investigation was about 8 mg. Although the crystals were produced in abundance, the difficulty of separating them from the matrix accounts for the small amount of pure crystals isolated. Even with these relatively pure crystals, it was exceedingly difficult to remove completely all the montmorillonite which clung to them with great tenacity. Therefore a good quantitative analysis was not obtained. However, a sample was analyzed by the Kem Tech Laboratories, Inc., Baton Rouge, Louisiana, using the Weiss ring oven. The analysis returned was sodium, 2.5%; calcium, 35.0%; aluminum, 5.0%; iron, 0.0%; and a strongly positive test for silicon. This method does not permit a quantitative determination for silicon.

A separate sample was analyzed for silica content only in the Department of Geology, Iowa State University. Unfortunately, this sample also contained impurities, but, based on the sample furnished silica content was determined to be 29.4%. Also, from the x-ray analysis discussed below, further doubt arises.

Based on the assumptions that (i) calcium occurs as CaO and silicon as SiO_2; (ii) sodium and aluminum are isomorphous substitutions for calcium and silicon, respectively; and (iii) the original materials mixed were montmorillonite, calcium hydroxide, and distilled water, the percent by weight of each constituent can be computed and then converted to molecular proportions. Percentages by weight of the constituents are CaO, 49.0%; NaO, 4.2%; AlO_2, 10.9%; SiO_2, 29.4%; and H_2O, 6.5%. Converting these to molecular proportions by dividing by the molecular weight of each constituent gives CaO plus NaO, .982; AlO_2 plus SiO_2, .675; and H_2O, .360. This gives a molecule of composition

$$3(Ca_{.89}Na_{.11})O \cdot 2(Si_{.73}Al_{.27})O_2 \cdot H_2O.$$

Because of the impurities contained in the samples, and because the analyses were not performed at the same time on a single sample by the same method, the accuracy of the analysis from a quantitative standpoint is questionable, though from a qualitative standpoint it has merit.

X-ray analysis

Comparison of the observed d-spacings and intensities with those in the x-ray powder data file (2) showed a striking resemblance between the diffraction data of this crystal and the data for two calcium aluminate hydrates: $4CaO \cdot Al_2O_3 \cdot xH_2O$ and $3CaO \cdot Al_2O_3 \cdot 8\text{-}12H_2O$. However, small variances in d-spacings and intensities do not permit positive identification with either of these two compounds.

A comparison with the data published by Wells (25) shows an even more striking resemblance between the powder pattern for these crystals and Wells' pattern for $4CaO \cdot Al_2O_3 \cdot 13H_2O$ though some intensity differences

still exist. In addition, Wells observed for the ordinary ray an index of refraction of 1.547 in a compound whose composition was $3.97CaO \cdot Al_2O_3 \cdot 13.04H_2O$. For crystals of similar composition, Roberts (22) determined a specific gravity of 2.02 for the 13 water hydrate and 2.08 for the 11 water hydrate. These compare closely with the values determined for the crystals studied in this paper where ω equals $1.548 \pm .002$ and the specific gravity is 2.07.

However, Wells indexed the crystal differently than was found to be the case here with the result that his unit cell was considerably different. His indexing was apparently based only on a powder film. During the course of this investigation, a similar set of indices was initially assigned to the crystal based only on a powder film. It was not until a single crystal rotation photograph was taken that it became apparent that only the basal reflections in multiples of six appeared with the others extinguished by a six-fold screw axis in the hexagonal cell.

On the basis of unit cell volume and density the C_4AH_{13} hypothesized formula would indicate a unit cell composed of three molecules since

$$N = \frac{\rho V A}{M} \qquad 19$$

where N = No. of molecules/unit cell

ρ = density (2.07 gms/cm^3)

V = unit cell volume ($133.82 \cdot 10^{-23} cm^3$)

A = Avogadro's No. ($6.025 \cdot 10^{23}$ molecules/mole)

and M = formula weight (560.49 gms/mole).

Then N = 2.97 3 molecules/unit cell.

This suggests the strong possibility that the unit cell is made up of alternating layers of calcium hydroxide and aluminum hydroxide.

Because of the strikingly similar physical, optical, chemical, and x-ray properties existing, these crystals must be nearly isostructural with $4CaO \cdot Al_2O_3 \cdot 13H_2O$. But, since the chemical analysis showed the presence of silicon and sodium also, and since some variation in intensities and d-spacings exist, a positive identification with this compound cannot be made. However, the deviations noted may be due to the incorporation of silica in the crystal structure or due to CO_2 in solid solution in the crystal.

CONCLUSIONS

1. In mixtures of lime, soil M-67, and water, which are moist cured for thirty days, a crystalline reaction product develops. This product is produced in optimum quantities at lime contents of 20 percent by dry weight of soil and at high moisture contents. Only the clay-size portion of the soil enters into the reaction.

2. The same crystalline reaction product develops in mixes of lime, water, and bentonite, but only after a considerably longer curing time is it produced in comparable quantities.

3. The crystals produced are transparent, colorless, platelike, and hexagonally shaped. Their density is $2.07 \pm .01$ gm/cm^3 at 70°F. Observations under the petrographic microscope prove them to be uniaxial negative with $\omega = 1.548 \pm .002$.

4. X-ray investigations of the crystal structure prove that it is the rhombohedral division of the hexagonal system in space group D_{3d}^6 ($R\bar{3}c$) or C_{3v}^6 (R3c). Intensities from powder camera films and indexing by Weissenberg methods establish the four strongest lines at 7.59 Å, 00·6; 2.87 Å, 11·0; 2.30 Å, 20·8; and 3.85 Å, 01·8 and 00·12. Lattice constants are $a_0 = 5.755$ Å and $c_0 = 46.65$ Å for the hexagonal cell and $a = 15.90$ Å and $\alpha = 20.85°$ for the rhombohedral cell.

5. The chemical composition of the crystal could not be precisely determined; however, the d-spacings indicate a structure similar to that for $4CaO \cdot Al_2O_3 \cdot 13\ H_2O$ and it is possible that this is the composition of the crystal. If so, previously recorded data of Wells, et al. (25) for indexing

and unit cell dimensions are in error and should be revised. The deviations appearing in the x-ray determinations may be the result of silica in the crystal structure or CO_2 in solid solution in the crystal.

RECOMMENDATIONS FOR FURTHER RESEARCH

In pursuing further the research begun here, the writer suggests that a thorough review of all available literature on the calcium aluminates and silicates be undertaken. The extent of literature is so voluminous, diversified, and in so many languages that it makes this a significant and difficult task. A good compendum of available literature is, at present, not available. Such a compendum, when published, would be in great demand by all engaged in research on Portland cement, lime, fly ash, and other related fields. Thus, this work could be undertaken as a thesis requirement for a Masters Degree.

Following this would come the laboratory research phase as part of the requirement for a higher degree. Areas for further research are (1) to produce a large enough quantity of absolutely pure crystals that a positive quantitative analysis can be made; (2) to determine by means of a Patterson synthesis and Fourier analysis the locations of all ions in the unit cell and construct a model thereof; (3) to determine the identity and other features of crystals produced in pozzolanic reactions occurring when lime is added to fly ash and to other pure clays.

ACKNOWLEDGMENTS

The Officers' Graduate Training Program of the U. S. Army Corps of Engineers enabled the writer to engage in the research described in this paper. Further funds made available by the Highway Research Board of the Iowa State Highway Commission contributed to the purchase of the necessary expensive and complex equipment used.

Dr. Richard L. Handy, Associate Professor of Civil Engineering, gave instruction and guidance on technical matters which were extensive in nature and contributed greatly to the research conducted. Dr. R. E. Rundle, Professor of Physics, contributed most generously of his time, knowledge, and equipment, and Dr. John Lemish, Professor of Geology, provided responsible handling of the silica analysis.

The writer is especially indebted to the guidance of Dr. D. T. Davidson, Professor of Civil Engineering, under whose supervision this research was conducted.

Finally, I thank my wife for allowing me to work and study at home while she occupied the children elsewhere and who put up with long and continued absences on many evenings while I was working at the laboratory. Without her encouragement and understanding (and typing prowess) this research would not have been completed.

REFERENCES

1. Azaroff, L. V. and Buerger, M. J. The powder method in x-ray crystallography. New York, N. Y., McGraw-Hill Book Co., Inc. 1958.

2. Bessey, G. E. The calcium aluminate and silicate hydrates. Symposium on the Chemistry of Cements, Stockholm. Proceedings 1938: 178-230. 1938.

3. Brindly, G. E., ed. Index to the x-ray powder data file. Am. Soc. for Test. Mat. Technical Publication 48-G. 1958.

4. Buerger, M. J. The photography of the reciprocal lattice. Cambridge, Mass., The Am. Soc. for X-ray and Electron Diffraction. 1944.

5. Buerger, M. J. X-ray crystallography. New York, N. Y., John Wiley and Sons, Inc. 1942.

6. Clare, K. E. and Cruchley, A. E. Laboratory experiments in the stabilization of clays with hydrated lime. Geotechnique 7: 97-111. 1957.

7. Crosby, R. L. Lime-fly ash ratio and admixture content versus strength of stabilized clayey soil. Unpublished M. S. Thesis. Ames, Iowa, Library, Iowa State University of Science and Technology. 1957.

8. Davidson, D. T. and Handy, R. L. Soil stabilization. In Woods, K. B., ed. Highway engineering handbook. pp. 21.98-21.123. New York, N. Y., McGraw-Hill Book Co., Inc. 1960.

9. Division of Engineer Laboratories. Hydration of portland pozzolan cement. U. S. Dept. Agr., Bureau of Reclamation, Div. of Engr. Lab. Report Pet-121. 1957.

10. Heller, L. and Taylor, H. F. W. Crystallographic data for the calcium silicates. London, England, Her Majesty's Stationery Office. 1956.

11. Hilt, G. H. and Davidson, D. T. Lime fixation in clayey soils. Hwy. Res. Bd. Bulletin No. 262. 1960.

12. Kasper, J. S. and Lonsdale, K., ed. International tables for x-ray crystallography. Vol. 2. Birmingham, England, The Kynoch Press. 1959.

13. Kerr, P. F., Main, M. S., and Hamilton, P. K. Occurrence and microscopic examination of reference clay mineral specimens. American Petroleum Institute, Preliminary Report 5. 1950.

14. Klems, G. J. Cylindrical powder cameras. Norelco Reporter 6: 82-86. 1959.

15. Klug, H. P. and Alexander, L. E. X-ray diffraction procedures. New York, N. Y., John Wiley and Sons, Inc. 1954.

16. Krumbein, W. C. and Pettijohn, F. J. Manual of sedimentary petrography. New York, N. Y., Appleton-Century-Crafts, Inc. 1938.

17. Iowa State University of Science and Technology. Engr. Exp. Sta. Screenings from the Soil Research Lab. Vol. 1, Nos. 5, 6. Sept.-Oct., Nov.-Dec. 1957.

18. Lipson, H. and Cochran, W. The determination of crystal structures. London, Eng., G. Bell and Sons, Ltd. 1957.

19. Michel, K., Buser, H. W., and Feitknecht, W. Über den mechanismus der bildung von calcium - aluminiumhydroxysalzen. Helvetica Chimica Acta 34: 119-128. 1951.

20. Mylius, C. R. W. Über Calciumaluminathydrate und deren doppelsalze. Acta Academiae Aboensis, Mathematica et Physica 7: 3-147. 1933.

21. National Lime Association. Lime stabilization of roads. National Lime Association Bulletin No. 323. 1954.

22. Roberts, M. H. New calcium aluminate hydrates. Journal of Applied Chemistry, 7: 543-546. 1957.

23. Rogers, A. F. and Kerr, P. F. Optical mineralogy. New York, N. Y., McGraw-Hill Book Co., Inc. 1942.

24. Smothers, W. J. and Chiang, Y. Differential thermal analysis. New York, N. Y., Chemical Publishing Co., Inc. 1958.

25. Wells, L. S., Clarke, W. F., and McMurdie, H. F. Study of the system CaO - Al_2O_3 - H_2O at temperatures of 21° and 90°C. Journal of Research of the National Bureau of Standards 30: 367-409. 1943.

APPENDIX A: REFLECTION DATA

Table 8. General hkl reflections

hkl	h+k+l	h+k	h+l	k+l	hkl	h+k+l	h+k	h+l	k+l
$2\bar{1}\bar{1}$	0	1	1	-2	$1\bar{2}2$	1	-1	3	0
$1\bar{1}2$	0	2	-1	-1	$2\bar{2}1$	1	0	3	-1
$\bar{1}2\bar{1}$	0	1	-2	1	$4\bar{1}1$	4	5	3	0
$\bar{2}1\bar{1}$	0	-1	-1	2	$1\bar{4}1$	4	5	0	3
$\bar{1}\bar{1}2$	0	0	1	1	$\bar{1}41$	4	3	0	5
$\bar{1}2\bar{1}$	0	-1	2	-1	$\bar{1}\bar{1}4$	4	0	3	5
$3\bar{1}2$	0	2	1	-3	$1\bar{1}4$	4	0	5	3
$2\bar{1}3$	0	3	-1	-2	$4\bar{1}1$	4	3	5	0
$1\bar{2}3$	0	3	-2	-1	321	6	5	4	3
$1\bar{3}2$	0	2	-3	1	231	6	5	3	4
$2\bar{3}1$	0	1	-3	2	132	6	4	3	5
$3\bar{2}1$	0	-1	-2	3	123	6	3	4	5
$3\bar{1}2$	0	-2	-1	3	213	6	3	5	4
$2\bar{1}3$	0	-3	1	2	312	6	4	5	3
$\bar{1}2\bar{3}$	0	-3	2	1	411	6	5	5	2
$\bar{1}3\bar{2}$	0	-2	3	-1	141	6	5	2	5
$\bar{2}3\bar{1}$	0	-1	3	-2	$11\bar{4}$	6	2	5	5
$3\bar{2}\bar{1}$	0	1	2	-3	$4\bar{3}1$	6	7	3	2
$4\bar{2}2$	0	2	2	-4	$3\bar{4}1$	6	7	2	3
$2\bar{2}4$	0	4	-2	-2	$\bar{1}43$	6	3	2	7
$2\bar{4}2$	0	2	-4	2	$\bar{1}34$	6	2	3	7
$\bar{4}22$	0	-2	-2	4	$3\bar{1}4$	6	2	7	3
$\bar{2}24$	0	0	2	2	$4\bar{1}3$	6	3	7	2
$\bar{2}42$	0	-2	4	-2	$5\bar{2}1$	6	7	4	1
$4\bar{1}3$	0	-3	1	-4	$\bar{2}51$	6	7	1	4
$3\bar{1}4$	0	4	-1	-3	$\bar{1}52$	6	4	1	7
$1\bar{3}4$	0	4	-3	-1	$1\bar{2}5$	6	1	4	7
$1\bar{4}3$	0	3	-4	1	$2\bar{1}5$	6	1	7	4
$3\bar{4}1$	0	1	-4	3	$5\bar{1}2$	6	4	7	1
$\bar{4}31$	0	-1	-3	4	$\bar{2}44$	6	2	2	8
$\bar{4}13$	0	-3	-1	4	$4\bar{2}4$	6	2	8	2
$3\bar{1}4$	0	-4	1	3	$61\bar{1}$	6	7	5	0
$1\bar{3}4$	0	-4	3	1	$5\bar{3}2$	6	8	3	1
$1\bar{4}3$	0	-3	4	-1	$3\bar{5}2$	6	8	1	3
$3\bar{4}1$	0	-1	4	-3	$\bar{1}6\bar{1}$	6	7	0	5
$4\bar{3}1$	0	1	3	-4	$\bar{1}61$	6	5	0	7
$2\bar{1}2$	1	3	0	-1	$\bar{2}53$	6	3	1	8
$1\bar{2}2$	1	3	-1	0	$\bar{2}35$	6	1	3	8
$\bar{2}21$	1	0	-1	3	$\bar{1}16$	6	0	5	7
$\bar{2}12$	1	-1	0	3	$1\bar{1}6$	6	0	7	5

Table 8. (continued)

hkl	h+k+l	h+k	h+l	k+l	hkl	h+k+l	h+k	h+l	k+l
$3\bar{2}5$	6	1	8	3	254	11	7	6	9
$5\bar{2}3$	6	3	8	1	245	11	6	7	9
$6\bar{1}1$	6	5	7	0	425	11	6	9	7
233	8	5	5	6	524	11	7	9	6
323	8	5	6	5	543	12	9	8	7
422	8	6	6	4	453	12	9	7	8
242	8	6	4	6	354	12	8	7	9
224	8	4	6	6	345	12	7	8	9
431	8	7	5	4	435	12	7	9	8
341	8	7	4	5	534	12	8	9	7
143	8	5	4	7	633	12	9	9	6
134	8	4	5	7	363	12	9	6	9
314	8	4	7	5	255	12	7	7	10
413	8	5	7	4	525	12	7	10	7
521	8	7	6	3	642	12	10	8	6
251	8	7	3	6	462	12	10	6	8
152	8	6	3	7	264	12	8	6	10
125	8	3	6	7	246	12	6	8	10
215	-8	3	7	6	426	12	6	10	8
512	8	6	7	3	624	12	8	10	6
432	9	7	6	5	732	12	10	9	5
342	9	7	5	6	651	12	11	7	6
243	9	6	5	7	561	12	11	6	7
234	9	5	6	7	372	12	10	5	9
324	9	5	7	6	273	12	9	5	10
423	9	6	7	5	165	12	7	6	11
433	10	7	7	6	156	12	6	7	11
343	10	7	6	7	237	12	5	9	10
244	10	6	6	8	327	12	5	10	9
424	10	6	8	6	516	12	6	11	7
532	10	8	7	5	615	12	7	11	6
352	10	8	5	7	723	12	9	10	5
253	10	7	5	8	732	12	10	9	5
235	10	5	7	8	651	12	11	7	6
325	10	5	8	7	741	12	11	8	5
523	10	7	8	5	471	12	11	5	8
631	10	9	7	4	174	12	8	5	11
361	10	9	4	7	147	12	5	8	11
163	10	7	4	9	417	12	5	11	8
136	10	4	7	9	714	12	8	11	5
316	10	4	9	7	822	12	10	10	4
613	10	7	9	4	282	12	10	4	10
542	11	9	7	6	831	12	11	9	4
452	11	9	6	7	381	12	11	4	9

Table 8. (continued)

hkl	h+k+l	h+k	h+l	k+l	hkl	h+k+l	h+k	h+l	k+l
183	12	9	4	11	853	16	13	11	8
138	12	4	9	11	583	16	13	8	11
318	12	4	11	9	385	16	11	8	13
813	12	9	11	4	358	16	8	11	13
643	13	10	9	7	538	16	8	13	11
463	13	10	7	9	835	16	11	13	8
364	13	9	7	10	277	16	9	9	14
346	13	7	9	10	727	16	9	14	9
436	13	7	10	9	765	18	13	12	11
634	13	9	10	7	675	18	13	11	12
644	14	10	10	8	576	18	12	11	13
464	14	10	8	10	567	18	11	12	13
752	14	12	9	7	657	18	11	13	12
572	14	12	7	9	756	18	12	13	11
275	14	9	7	12	677	20	13	13	14
257	14	7	9	12	767	20	13	14	13
527	14	7	12	9	866	20	14	14	12
725	14	9	12	7	686	20	14	12	14
833	14	11	11	6	875	20	15	13	12
383	14	11	6	11	785	20	15	12	13
654	15	11	10	9	587	20	13	12	15
564	15	11	9	10	578	20	12	13	15
465	15	10	9	11	758	20	12	15	13
456	15	9	10	11	857	20	13	15	12
546	15	9	11	10	965	20	15	14	11
645	15	10	11	9	695	20	15	11	14
655	16	11	11	10	596	20	14	11	15
565	16	11	10	11	569	20	11	14	15
466	16	10	10	12	659	20	11	15	14
646	16	10	12	10	956	20	14	15	11
754	16	12	11	9	488	20	12	12	16
574	16	12	9	11	848	20	12	16	12
475	16	11	9	12	974	20	16	13	11
457	16	9	11	12	794	20	16	11	13
547	16	9	12	11	497	20	13	11	16
745	16	11	12	9	479	20	11	13	16
763	16	13	10	9	749	20	11	16	13
673	16	13	9	10	947	20	13	16	11
376	16	10	9	13	1055	20	15	15	10
367	16	9	10	13	5105	20	15	10	15
637	16	9	13	10	1064	20	16	14	10
736	16	10	13	9	6104	20	16	10	14
844	16	12	12	8	4106	20	14	10	16
484	16	12	8	12	4610	20	10	14	16

Table 8. (continued)

hkl	h+k+l	h+k	h+l	k+l	hkl	h+k+l	h+k	h+l	k+l
6410	20	10	16	14	895	22	17	13	14
1046	20	14	16	10	598	22	14	13	17
983	20	17	12	11	589	22	13	14	17
893	20	17	11	12	859	22	13	17	14
398	20	12	11	17	958	22	14	17	13
389	20	11	12	17	1066	22	16	16	12
839	20	11	17	12	6106	22	16	12	16
938	20	12	17	11	987	24	17	16	15
876	21	15	14	13	897	24	17	15	16
786	21	15	13	14	798	24	16	15	17
687	21	14	13	15	789	24	15	16	17
678	21	13	14	15	879	24	15	17	16
768	21	13	15	14	978	24	16	17	15
867	21	14	15	13	1088	26	18	18	16
877	22	15	15	14	8108	26	18	16	18
787	22	15	14	15	1097	26	19	17	16
976	22	16	15	13	9107	26	19	16	17
796	22	16	13	15	7109	26	17	16	19
697	22	15	13	16	7910	26	16	17	19
679	22	13	15	16	9710	26	16	19	17
769	22	13	16	15	1079	26	17	19	16
967	22	15	16	13					
985	22	17	14	13		ln	ln	ln	ln

Table 9. h01 reflections

h01	h	l	h+l	h01	h	l	h+l
$10\bar{1}$	1	-1	0	302	3	2	5
$\bar{1}01$	-1	1	0	303	3	3	6
$20\bar{2}$	2	-2	0	204	2	4	6
$\bar{2}02$	-2	2	0	402	4	2	6
$30\bar{3}$	3	-3	0	105	1	5	6
$\bar{3}03$	-3	3	0	501	5	1	6
102	1	2	3	404	4	4	8
201	2	1	3	305	3	5	8
202	2	2	4	503	5	3	8
103	1	3	4	505	5	5	10
301	3	1	4	606	6	6	12
203	2	3	5	507	5	7	12

Table 9. (continued)

h01	h	l	h+l
705	7	5	12
	ln	ln	ln

Table 10. 0kl reflections

0kl	k	l	k+l	0kl	k	l	k+l
$01\bar{1}$	1	-1	0	033	3	3	6
$0\bar{1}1$	-1	1	0	042	4	2	6
$02\bar{2}$	2	-2	0	024	2	4	6
$0\bar{2}2$	-2	2	0	051	5	1	6
$03\bar{3}$	3	-3	0	015	1	5	6
$0\bar{3}3$	-3	3	0	044	4	4	8
021	2	1	3	053	5	3	8
012	1	2	3	035	3	5	8
022	2	2	4	055	5	5	10
031	3	1	4	066	6	6	12
013	1	3	4	075	7	5	12
032	3	2	5	057	5	7	12
023	2	3	5				
					ln	ln	ln

Table 11. hk0 reflections

hk0	h	k	h+k	hk0	h	k	h+k
$\bar{1}10$	-1	1	0	130	1	3	4
$1\bar{1}0$	1	-1	0	320	3	2	5
$\bar{2}20$	-2	2	0	230	2	3	5
$2\bar{2}0$	2	-2	0	420	4	2	6
$\bar{3}30$	-3	3	0	240	2	4	6
$3\bar{3}0$	3	-3	0	510	5	1	6
210	2	1	3	150	1	5	6
120	1	2	3	530	5	3	8
310	3	1	4	350	3	5	8

Table 11. (continued)

hk0	h	k	h+k	hk0	h	k	h+k
750	7	5	12	570	5	7	12
					1n	1n	1n

Table 12. hhl reflections

hhl	h	l	h+l	2h+l	hhl	h	l	h+l	2h+l
$11\bar{2}$	1	-2	-1	0	556	5	6	11	16
$\bar{1}\bar{1}2$	-1	2	1	0	664	6	4	10	16
$22\bar{4}$	2	-4	-2	0	448	4	8	12	16
$\bar{2}\bar{2}4$	-2	4	2	0	772	7	2	9	16
$44\bar{2}$	4	-2	2	6	776	7	6	13	20
332	3	2	5	8	668	6	8	14	20
224	2	4	6	8	884	8	4	12	20
334	3	4	7	10	5510	5	10	15	20
442	4	2	6	10	778	7	8	15	22
552	5	2	7	12	6610	6	10	16	22
336	3	6	9	12	8810	8	10	18	26
228	2	8	10	12					
						1n	2n	1n	2n

(110) glide plane, component $\frac{c}{2}$

Table 13. hh0 reflections

hh0	h	hh0	h
220	2	550	5
330	3	660	6
440	4		
			1n

Table 14. h00, 0k0, and 001 reflections

h00	h	0k0	k	001	1
200	2	020	2	002	2
600	6	060	6	006	6
	2n		2n		2n

$[100]$, $[010]$, and $[001]$ screw axes, component $\frac{a}{2}$

APPENDIX B: OTAY BENTONITE DATA

Table 15. Occurrence and composition

Formula: $(Al_{1.43}Fe_{.03}Mg_{.64})(Al_{.01}Si_{3.99})O_{10}(OH)_2(Na_{.12}Ca_{.07})$

Type: Dioctahedral

Impurities: 4%

Quartz: 1%

Orthoclase: 0.5-1%

Sericite: 1-2%

Limonite and dark minerals: Traces

Epoch: Pliocene

Overburden: Sandstone and soil, 10 feet
